Fibers and Polymers 2022, Vol.23, No.3, 699-710
DOI 10.1007/s12221-022-3393-z

ISSN 1229-9197 (print version)
ISSN 1875-0052 (electronic version)

Preparation and Characterization of Pullulan/Tempo Cellulose Nanofibril/Ag Nanocomposite Film for Antimicrobial Food Packaging Application

Sabina Yeasmin[1], Il Jun Kwon[2], Dong Jun Kwon[3], Jungeon Lee[1], Jeong Hyun Yeum[1]*, Byung Chul Ji[4], Jae Min Park[1], and Seong Baek Yang[1]*

[1]*Department of Biofibers and Biomaterials Science, Kyungpook National University, Daegu 41566, Korea*
[2]*Industrial Materials R&D Group, DYETEC Institute, Daegu 41706, Korea*
[3]*Research Institute for Green Energy Convergence Technology, Gyeongsang National University, Jinju 52828, Korea*
[4]*Department of Textile System Engineering, Kyungpook National University, Daegu 41566, Korea*
(Received December 10, 2020; Revised March 24, 2021; Accepted May 2, 2021)

Abstract: In this study, pullulan (PULL) nanocomposite films containing tempo cellulose nanofibrils (TOCNs) and Ag nanoparticles were successfully prepared using a solution casting technique in aqueous solutions. X-ray diffraction results and optical microscopy images revealed the coexistence of Ag and PULL/TOCNs blend matrix as well as the uniform distribution of Ag nanoparticles. The Fourier-transform infrared data showed that a good interaction occurred between TOCNs, Ag, and PULL matrix; the prepared composite film showed improved characteristics including higher tensile strength, thermal stability, water barrier properties and reduced moisture susceptibility compared to a neat PULL film. In addition, the prepared film is biodegradable and possesses antimicrobial characteristics. These excellent properties clearly indicate that this type of ternary nanocomposite film may have prospective food packaging and medical application.

Keywords: Pullulan, Tempo cellulose nanofibrils, Silver, Nanocomposite film, Biodegradability

Introduction

Pullulan (PULL) is a non-ionic, non-toxic, and non-carcinogenic exopolysaccharide generated by the fungus-like yeast *Aureobasidium pullulans*; PULL exhibits excellent characteristics including biodegradability, biocompatibility, and water solubility [1] and has a considerable potential for use in a multitude of fields, e.g., food packaging [2], tissue engineering [3], and drug and gene targeting [4]. Motivated by the extraordinary film-forming ability of PULL and its excellent properties (e.g., tastelessness, odorlessness, transparency, heat stability, oxygen impermeability), many publications related to PULL-based films and coatings for food packaging have been published in the previous decades [2,5-15].

Cellulose, the richest and renewable carbon source in the world, exists in nature in a fibrous crystal condition, named cellulose microfibril; cellulose is frequently used as a sustainable supporting material [16]. Owing to high aspect ratios [17] and high elastic moduli [18], cellulose microfibril can be used to fabricate composite materials with superior transparency and extraordinary mechanical properties. The combination of conventional polymers with plant cellulose nanofibrils, e.g., micro-fibrillated celluloses (MFCs) [18-21] and nanocrystalline celluloses or cellulose nanowhiskers [22-27] obtained by the sulfuric acid treatment, has been intensively investigated in recent years. However, owing to disadvantages (e.g., MFCs contain bunches of cellulose nanofibrils, and cellulose nanowhiskers show comparatively low aspect ratios (~50) [23,28], sometimes filler incorporation of >10 wt.% is needed to achieve considerable reinforcement of polymer matrices. To overcome this problem, cellulose nanofibrils with high aspect ratios can be separated from wood celluloses using 2,2,6,6-tetramethylpiperidine-1-oxyl (TEMPO)-mediated oxidation followed by mild mechanical action in water [19,27]. This type of TEMPO-oxidized cellulose nanofibrils (TOCNs) exhibits extraordinary properties including uniform widths (3-4 nm), high aspect ratios of more than 100 [19-21], and high elastic moduli [145 GPa] [22]. Consequently, TOCNs allow achieving a more efficient reinforcement in polymer matrices compared to usual cellulosic nanomaterials. Several TOCNs/polymer composites have been described in previous papers [23,24, 26,28,29].

An antimicrobial packaging technique has been established as one of the most promising active packaging methods which help to advance food safety and expand the shelf life of food by defeating or reducing spoilage and pathogenic microorganisms that pollute foods [30,31]. Nanocomposite systems with antimicrobial performance are especially efficient owing to the high surface-to-volume ratio and improved surface reactivity of nanosized antimicrobial particles, which makes them capable of destroying more microorganisms compared to other higher scale counterparts [29]. Many nanoparticles or nanocomposite materials have been examined for their antimicrobial performance [32-36].

Nanocomposites with an antimicrobial function are extremely useful for decreasing the growth of post-processing pollutant microorganisms, prolonging the shelf life of food, and increasing food safety. One of the greatest broadly studied nanocomposites applied as antimicrobial

*Corresponding author: jhyeum@knu.ac.kr
*Corresponding author: ysb@knu.ac.kr

food packaging is based on silver nanoparticles (AgNPs) included into polymeric films [29,35,37,38]. This occurs mostly owing to the effective antimicrobial action of silver against a large variety of bacteria, viruses, and fungi [39,40] as well as their exceptional physicochemical characteristics. The antimicrobial role of silver is mostly attributed to the function of silver ions and metallic silver nanoparticles. AgNPs are used for the preparation of antimicrobial packaging films owing to their powerful antimicrobial activity with high stability [41].

The use of neat PULL films is not suitable for packaging applications owing to their hydrophilic character, brittleness, and lack of active function. The use of PULL-based blends and composite films is an effective approach to solve these core limitations and gain multifunctional packaging utility to increase shelf life, protection, and food quality [42]. Several PULL-based composite films have been reported [e.g., PULL/alginate [43], PULL/Ag and essential oil [44], PULL/lysozyme nanofibers [42], PULL/bacterial cellulose [13], PULL/graphene oxide [14]. A schematic diagram of the preparation of PULL/TOCNs/Ag nanocomposite films and their biodegradation process and antimicrobial effectiveness are shown in Figure 1.

To our knowledge, there are no studies on the use of Ag/TOCNs hybrid fillers in PULL. In addition, in this study, we studied the biodegradability of the PULL/TOCNs/Ag composite film by the soil burial method, which has not been performed in other studies on the PULL/Ag composite. TOCNs are a potentially natural reinforcing agent in preparing polymer nanocomposites, and several studies have been performed to show the dispersibility, morphology and effect of TOCNs content in preparing polymer composites [45,46]. Herein, from our preliminary study, the optimized concentration of TOCNs (5 wt.%) is kept constant [47,48] and the effects of various Ag contents on mechanical, thermal, morphological, and antimicrobial properties of PULL/TOCNs/Ag hybrid nanocomposites films prepared by the solution casting method have been examined. The main reason for the incorporation of Ag into PULL/TOCNs nanocomposites is to increase the mechanical and thermal properties and to develop the antimicrobial properties of nanocomposite films, which are important properties of packaging materials.

Experimental

Materials

A food-grade preparation of pullulan powder (purity= above 90 %, M_w=20,000) was supplied by Hayashibara Biochemical Laboratories Inc. (Okayama, Japan). The silver

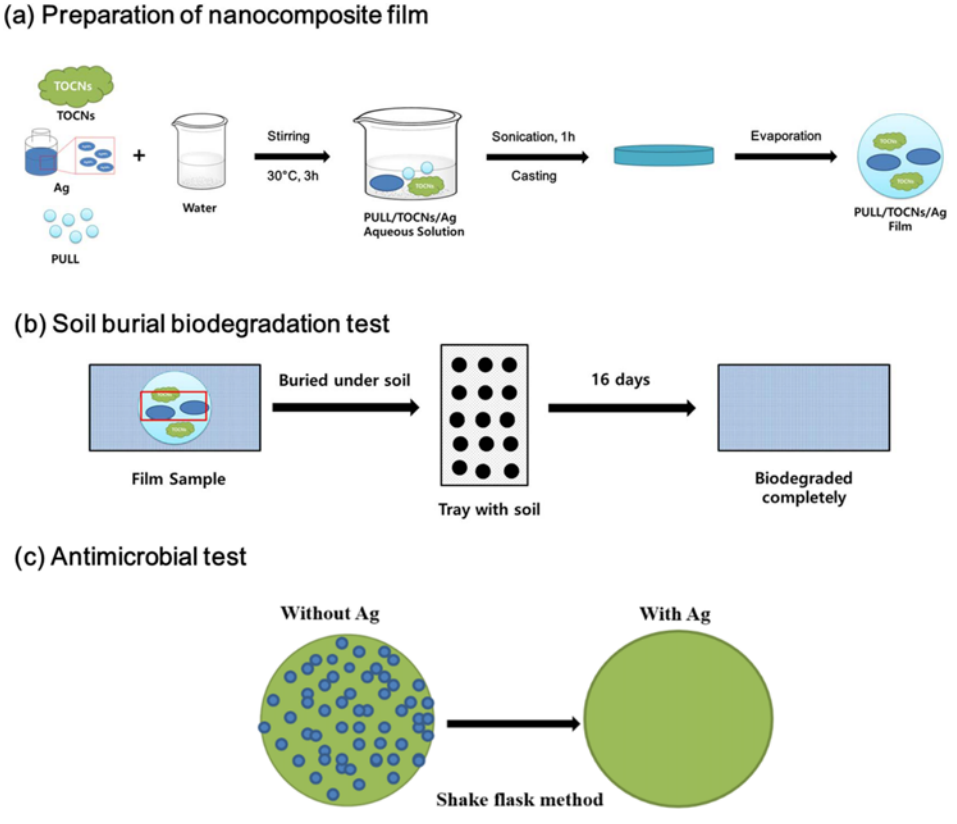

Figure 1. Schematic illustration of the parts of the experiment; (a) preparation of nanocomposite film, (b) soil burial biodegradation test, and (c) preservation test.

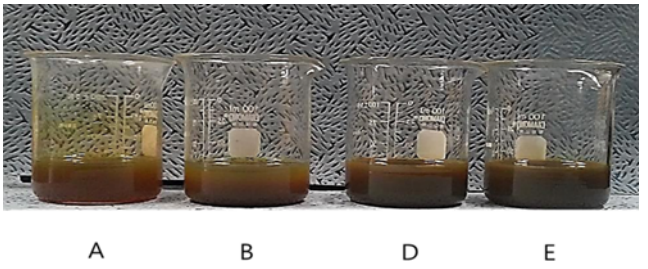

Figure 2. Photograph of the blend solutions; (A) PULL/TOCNs/Ag 0.5 wt.%, (B) PULL/TOCNs/Ag 1 wt.%, (C) PULL/TOCNs/Ag 3 wt.%, and (D) PULL/TOCNs/Ag 5 wt.%.

nanoparticle aqueous dispersion (AGS-WP001, 10,000 ppm) containing particles with the diameters of ca. 15-30 nm was bought from Miji Tech., Korea. Tempo cellulose nanofibrils (TOCNs) (aqueous 0.5 % w/v suspensions) were bought from Sigma-Aldrich. Double-distilled water was used to make all solutions.

Preparation of PULL/TOCNs/Ag Blend Solutions

First, TOCNs was added to double-distilled water and dissolved under magnetic stirring up to 1 h at room temperature. Then, an aqueous dispersion of AgNPs was added into the TOCNs solution and stirring continued to complete dispersion. Finally, a pullulan powder was incorporated into the same solution, and stirring continued until the powder dissolved. Finally, the prepared blend was homogenized for 1 h using a 750-W probe sonicator (20 %, Vibra-Cell Sonics) to ensure proper AgNPs dispersion. Here, 10 wt.% pullulan (on the basis of solution weight), 5 wt.% TOCNs (on the basis of pullulan weight), and an aqueous dispersion of AgNPs with various AgNPs contents [0, 0.5, 1, 3 and 5 wt.% (on the basis of PULL weight)] were used to prepare the PULL/TOCNs/Ag solution. The photograph of PULL/TOCNs/Ag blend solutions is shown in Figure 2.

Preparation of PULL/TOCNs/Ag Nanocomposite Films by the Solution Casting Method

The PULL/TOCNs/Ag composite film was made by casting it into crystal grade polystyrene petri dish molds at room temperature. Finally, after the complete drying of solution, the films were pulled out and preserved in a plastic bag for characterization. The photograph of film samples and the thickness of PULL/TOCNs/Ag nanocomposite films are shown in Figure 3 and Table 1, respectively.

Short-term Thermal Exposure of Nanocomposite Films

The short-term thermal exposure test was conducted according to reference [49]. Prior to heat exposure in air, oven samples (20×20 mm) were kept under ambient conditions (23 °C and 50 % R.H.) for 96 h. The oven (Vision Scientific Co., Ltd., VS-4172D) was circulated with air to prevent oxygen depletion. At least three samples for each condition were studied. Here, temperature up to 100 °C was chosen for heat exposure, by considering real applications.

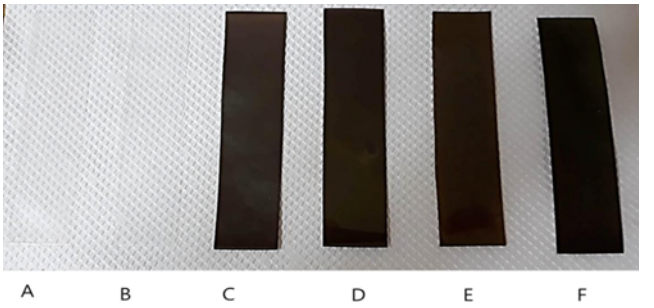

Figure 3. Photographs of the film samples; (A) PULL, (B) PULL/TOCNs, (C) PULL/TOCNs/Ag 0.5 wt.%, (D) PULL/TOCNs/Ag 1 wt.%, (E) PULL/TOCNs/Ag 3 wt.%, and (F) PULL/TOCNs/Ag 5 wt.%.

Table 1. Thickness of PULL/TOCNs/Ag nanocomposite films

Sample	Thickness (μm)
PULL	150±4.12
PULL/TOCNs	150±5.23
PULL/TOCNs/Ag 0.5 %	151±3.06
PULL/TOCNs/Ag 1 %	153±2.18
PULL/TOCNs/Ag 3 %	155±4.09
PULL/TOCNs/Ag 5 %	155±3.29

Preservation Test

The preservation efficacy of PULL/TOCNs/Ag hybrid films was tested to assess their antimicrobial characteristics [50]. The films were dispersed in a viscous solution of 0.01 wt.% of neutral polyacrylic acid (Carbopol 941, Noveon Inc.). The combined culture of microorganisms, named *Staphylococcus aureus* (ATCC6538) and *Escherichia coli* (ATCC25922), was grown in a tryptone soy broth at 32 °C for 24 h. Then, 0.2 g of microorganism suspensions and 20 g of samples were inoculated to make the initial bacteria concentration of 10^6 cfu/g. Then, the inoculants and samples were homogeneously mixed and preserved at 32 °C. Finally, the microbes were counted according to the pour plate count method.

Soil Burial Test

Soil burial test was performed on a laboratory scale [51] to explore the biodegradability of the film in a qualitative system. An aluminum tray was filled with compost soil; the film pieces (2 cm×2 cm) were buried bellow 4 cm from the soil surface to ensure aerobic degradation. Water was sprayed twice a day to moisten the compost. At various times, a sample of each film was unburied, oven-dried at the temperature of 30 °C for 24 h, and a picture was captured to

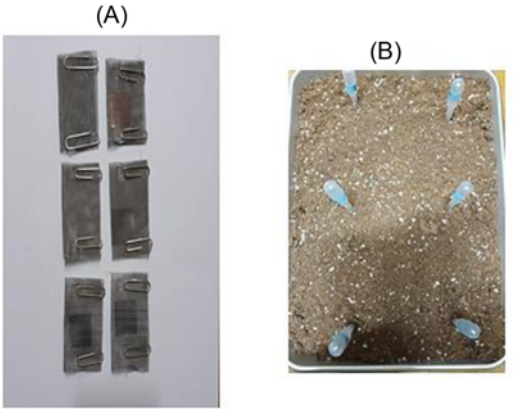

Figure 4. Photograph of the (A) film samples inside the iron mesh and the (B) tray used for the soil burial test.

note its degradation. Photographs of the film sample inside an iron mesh and tray used for the soil burial test are shown in Figure 4.

Characterization of the Films

The film thickness was quantified using a thickness gage (IP65, Mitutoyo, Takatsu-ku, Japan). An optical microscope was used to observe the surface morphology of the PULL/TOCNs/Ag composites films. To inspect the surface roughness of PULL/TOCNs/Ag nanocomposite films, atomic force microscopy [AFM, Park Systems (NX20), Mannheim, Germany] was used. In addition, film characterization was done using Fourier-transform infrared (FT-IR) spectroscopy (Frontier, Perkin Elmer, Waltham, MA, USA), and X-ray diffraction (XRD) (D/Max-2500, Rigaku, Tokyo, Japan). The thermal stability of films was examined with the thermogravimetric analysis (TGA) (modelQ-50; TA Instruments, USA) method. TGA tests were completed in a nitrogen gas atmosphere at the heating rate of 10 °C/min in the temperature range from ambient to 600 °C. Using differential scanning calorimetry (DSC) (DSC Q2000, TA Instruments, and New Castle, DE, USA), the crystal melting temperature of PULL/TOCNs/Ag nanocomposite films was examined. In addition, according to reference [49], a short-term thermal exposure test was done. The biodegradability behavior of PULL/TOCNs/Ag nanocomposite films was examined using the soil burial method [52-55].

The antibacterial functions were examined to observe the biological function of PULL/TOCNs/Ag nanocomposites films by KSM 0146 (a shake flask method) using ATCC 6538 (*Staphylococcus aureus*) and ATCC 25922 (*Escherichia coli*).

Tensile Strength

The mechanical characteristics were examined using an Instron 5567 universal testing machine (20-mm/min crosshead speed and 500-N load cell) according to ASTM D638-96. Film specimens (20×60 mm in size) were prepared for this test, and a minimum of three specimens were examined for each sample.

Optical Properties

Using UV/vis spectroscopy (K Lab Co., Ltd., OPTIZEN 2120UV) the light transmittance of PULL and PULL/TOCNs/Ag (0-5 wt.%) was measured. The film average thickness was 0.15 mm, and the wavelength range and scan interval were 200-800 nm and 10 nm, respectively. Air was used as a reference.

Water Contact Angle

The water contact angle was determined using the sessile drop method and a digital optical camera (Dino-Lite, AM7013MZT). A total of 4 μ*l* of water was put on each sample (2×2 cm^2) at room temperature. After the addition of the liquid drop, the contact angle was measured within 20 s. Snapshots were recorded at 0 s. For each sample, the contact angle was calculated.

Moisture Uptake

To measure the moisture uptake (Mu), film samples were placed in a locked atmospheric equilibrium at the R.H. of 68 % using $CuCl_2$ (saturated) solutions for 10 d. For each type of film, three samples were used. After reaching equilibrium, the equilibrated weights of film samples were recorded as W_1; after 4 h of drying in an oven, the samples were weighed again, and the weight was records as W_2. After achieving equilibrium, the equilibrated weights of the samples were recorded as W_1. Then, the films were dried in an oven at 100 °C for at least 4 h and weighed again (W_2). Water percentages were calculated using the following equation:

$$Mu\ (\%) = (W_1 - W_2)/W_2$$

Results and Discussion

Dispersion of Nanofillers in PULL-based Films

Optical Microscopy Analysis

An optical microscopy images were acquired to observe the detailed morphology of PULL/TOCNs/Ag nanocomposite films (Figure 5). This figure shows that differences of film morphology are clearly visible in the PULL/TOCNs/Ag (0-5 wt.%) film structure when the Ag content increases (Figures 5c-f). The images of the films (Figures 5c-d) show that even at low Ag content (0.5-1 wt.%), there was a uniformly homogeneous filler distribution in the PULL matrix. However, the nanocomposites dispersed with AgNPs of the 3-5 wt.% (Figures 5e, f) had a large amount of AgNPs dispersed in the PULL matrix with a change of morphology such as few agglomerates, voids, etc. compared to the film morphology with AgNPs content of 0.5-1 wt.%.

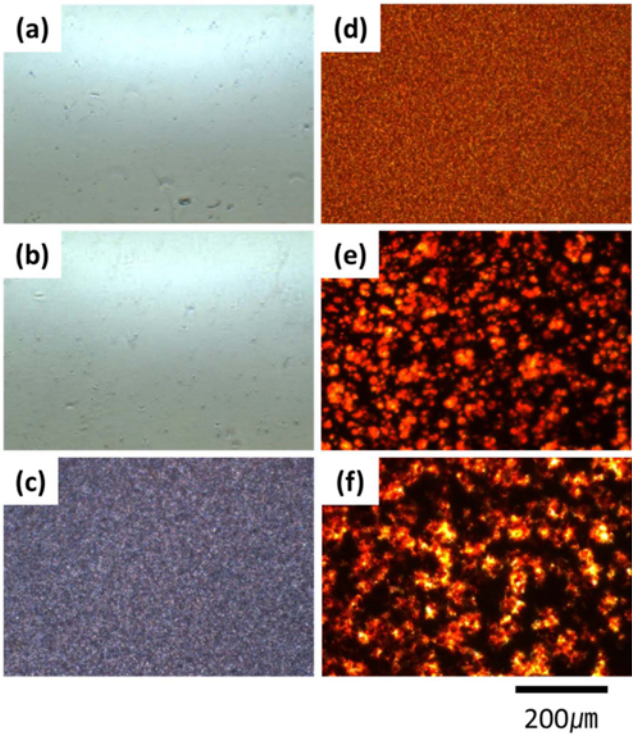

Figure 5. OM images of the film samples; (a) PULL, (b) PULL/TOCNs, (c) PULL/TOCNs/Ag 0.5 wt.%, (d) PULL/TOCNs/Ag 1 wt.%, (e) PULL/TOCNs/Ag 3 wt.%, and (f) PULL/TOCNs/Ag 5 wt.%, (PULL concentration=10 wt.%, TOCNs concentration= 5 wt.%).

This result indicates the sufficient distribution and dispersion of Ag in the PULL matrix by the sonicator. In addition, due to the homogenous dispersion of Ag in the PULL/TOCNs matrix, it was partly exposed to the outside and roughed it up and matrix cannot be seen on the surface (Figures 5c-f) [56].

AFM Analysis

AFM was used to describe the surface topographic aspect of the film. Figure 6 shows the surface plots from the height signal for PULL and PULL/TOCNs/Ag nanocomposite films. As usual, the surface roughness of PULL/TOCNs/Ag 5 wt.% nanocomposite film is higher (Rq=1.020 nm) than that of PULL (Rq=0.282 μm), which is similar to the OM results (Figure 5f). It is determined that the presence of AgNPs on the film results in a less homogeneous surface than that of the film without AgNPs owing to their coagulation nature.

FT-IR Analysis

The structure of neat PULL and PULL/TOCNs/Ag (0, 0.5, 1, 3, and 5 wt.%) composite films is determined by FT-IR spectra in the 500-4000 cm^{-1} range. Neat PULL films exhibited identical bands, as shown in Figure 7a. A strong peak at 850 cm^{-1} represents α-glucopyranose units. The peaks at 755 cm^{-1} and 932 cm^{-1} confirmed the presence of α-

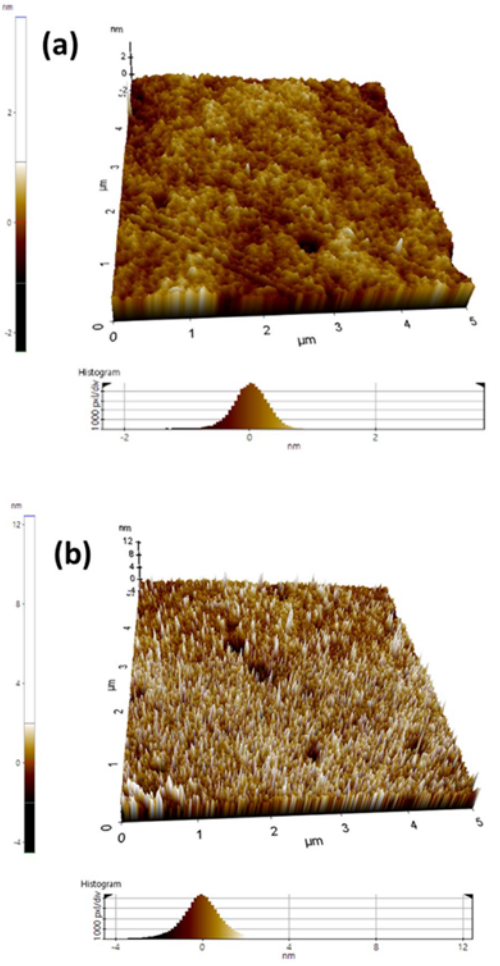

Figure 6. AFM images of the film samples; (a) PULL and (b) PULL/TOCNs/Ag 5 %. The values of Rq (nm) are (a) 0.282 and (b) 1.020 (PULL concentration=10 wt.%, TOCNs concentration= 5 wt.%).

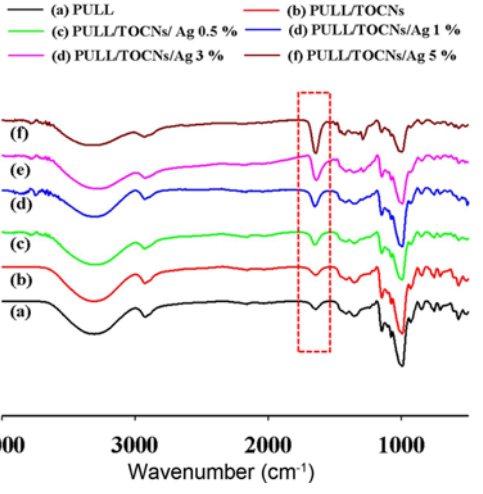

Figure 7. FT-IR data of neat PULL and PULL/TOCNs/Ag composite films with various Ag contents (0-5 wt.%). (TOCNs concentration=5 wt.%, PULL concentration=10 wt.%).

(1, 4) glycosidic and α-(1, 6) glycosidic bonds, respectively. Furthermore, the frequencies are the same for the reference and estimated samples [57]. The stretching vibration bands of CH and CH_2 groups are observed at 2850-3000 cm^{-1}, and vibrations bands in the 1300-1500 cm^{-1} range are attributed to CH/CH_2 deformation. In addition, a broad hydroxyl band was observed at 3000-3600 cm^{-1}, and C-O stretching was confirmed by the peak at 1000-1260 cm^{-1}.

The spectra for neat pullulan and those for the PULL/TOCNs/Ag (0-5 wt.%) film sample exhibited similar characteristics (Figures 7a-f). These results established a similar chemical structure of the samples. For PULL/TOCNs, the peak intensity of some peaks (3000-3600 cm^{-1}, 2850-3000 cm^{-1}, 1644 cm^{-1}, etc) slightly increased (Figure 7b). This result was obtained possibly owing to the interaction that happened between PULL and TOCNs by the hydrogen bonding of unsubstituted chain because both of them contained monosaccharide units that were joined by a (1→4) glycosidic bond [58-60]. After the addition of AgNPs to PULL/TOCNs, the peak intensity changed owing to this reinforcing element.

Low-intensity carbonyl band is observed at 1644 cm^{-1} in PULL, and its intensity gradually increases after the addition of Ag fillers. All bands that exist in PULL/TOCNs composites also exist in PULL/TOCNs/Ag composites (Figures 7b-f). The small shifts in absorption maximum and the difference in band shape are due to the deviation in the nearby functional groups. These types of interpretations are demonstrated for bands that exist in the 1000-1750 cm^{-1} region. Therefore, FT-IR spectroscopy confirmed the interactions that possibly occurred between the PULL matrix and AgNPs.

XRD Analysis

Figure 8 shows the XRD patterns of neat PULL and PULL/TOCNs/Ag (0, 0.5, 1, 3, and 5 wt.%) nanocomposites films. A broad peak was obtained at 19.4 °, which was attributed to the d-spacing of 4.52 ° for neat PULL [61]. In addition, the addition of cellulose nanofibrils into PULL results in the development of characteristic diffraction peaks of cellulose I (native cellulose) at 2θ 14.3, 15.9, 22.6, and 33.7; however, at low concentration (~5 wt.%) [12], intensity is reduced and the peaks cannot be differentiated (Figure 8A). Except for the diffraction peaks of the PULL/TOCNs blend, all other peaks are due to the silver phase (Figures 8B: c-f). These peaks are attributed to the (1 1 1) and (2 0 0) planes of silver nanocrystals with cubic symmetry [62]. Generally, the existence of small particles as filler is responsible for the decrease of polymer crystallinity because small filler particles interrupt the reassociation of the chain. Here, the intensity of peaks (19.4 °) of the PULL/TOCNs also decrease with the addition of the nanofiller [Ag (0.5-5 %)] because of the dispersion of AgNPs in the PULL/TOCNs blend matrix as well as the interaction of AgNPs with the PULL/TOCNs blend which improved the thermal, mechanical, and antibacterial activity of PULL/TOCNs/Ag nanocomposites as will be seen later in this research [63].

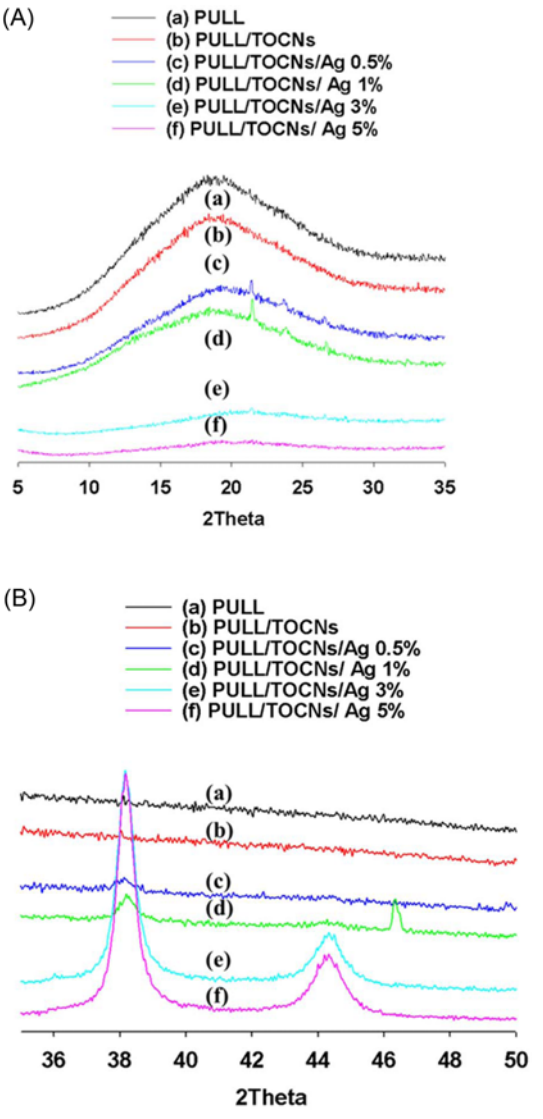

Figure 8. XRD data of neat PULL and PULL/TOCNs/Ag composite films with various Ag contents (0-5 wt.%) ranging (A) from 5 to 35 degree and (B) from 36 to 50 degree (TOCNs concentration=5 wt.%, PULL concentration=10 wt.%).

Thermal Properties of PULL/TOCNs/Ag Nanocomposite Films

DSC Analysis

Melting transition of the PULL/TOCNs/Ag film is determined by DSC at different Ag contents. Figure 9 shows the DSC thermograms of PULL/TOCNs/Ag films with a different content of AgNPs (0.5 wt.% and 5 wt.%) on the basis of polymer weight and the polymer concentration of 10 wt.%. The peak of melting transition for PULL/TOCNs/Ag 0.5% changes from 105 °C to 110 °C for 5 wt.% of

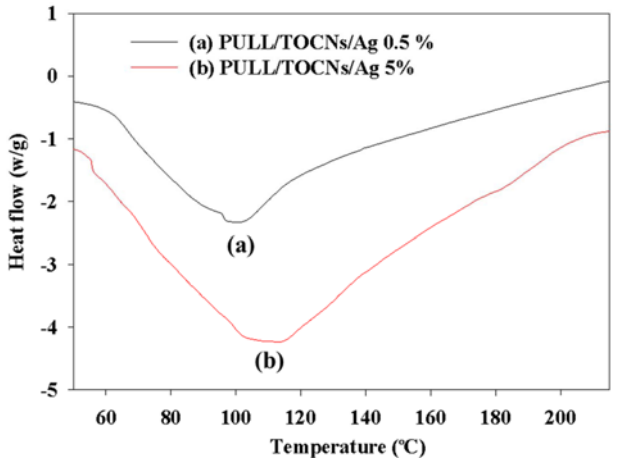

Figure 9. DSC data of PULL/TOCNs/Ag composite films with various Ag contents (0.5 and 5 wt.%). (TOCNs concentration= 5 wt.%, PULL concentration=10 wt.%).

AgNPs. Thus, with the addition of AgNPs, the thermal properties improved. This result suggests a very strong interaction between the PULL chains and AgNPs. This result is supported by other studies [64]. In the case of some amorphous polymer like PULL, DSC results do not show crystallization peak because the rate of nucleation and growth is extremely slow. Contradictory results have been reported for the explanation of this thermal event; previous studies reported that, as pullulan is amorphous in nature, it illustrates a range of melting temperatures, with endothermic transitions rather than a clear melting point [65].

TGA Analysis

The thermal stability of the PULL/TOCNs/Ag composite film with the Ag content of 0, 1, 3, and 5 wt.% (on the basis of polymer concentration) and 5 wt.% TOCN concentration on the basis of polymer concentration and 10 wt.% total polymer concentration was determined using the TGA analysis system in a nitrogen atmosphere (Figure 10). The thermal stability slightly increased for the PULL/TOCNs composite film even without adding Ag in the polymer blends of the composite films. In the temperature range of 300-500 °C, the highest curve is for the composite film with 5 wt.% of Ag, and the lowest curve is for PULL. The films with high AgNPs content exhibit high thermal stability, which may be due to the higher chain compactness that exists in the polymer blend attributed to the interaction that happened between the PULL/TOCNs blend and AgNPs [66]. Up to 225 °C, the thermal property improves from PULL to PULL/TOCNs/Ag 5 %.

Short-term Thermal Exposure

To obtain an additional information about the film's thermal degradation process, the color and weight of the sample were investigated. Before thermal exposure, the film samples were kept in a standard atmosphere (23 °C and

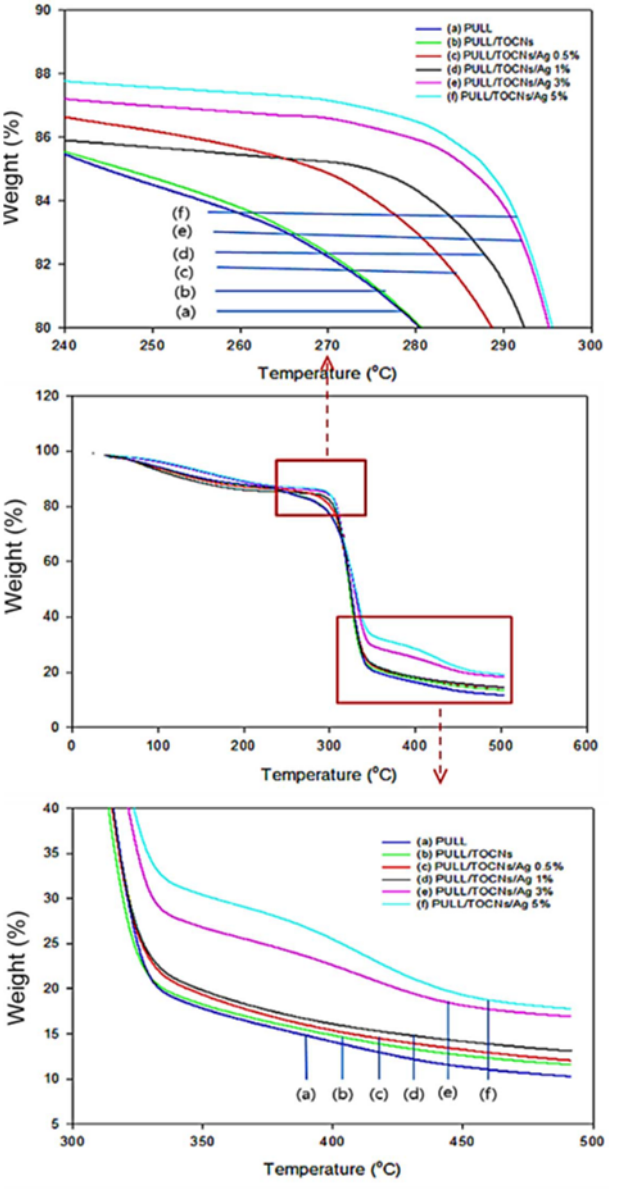

Figure 10. TGA data of neat PULL and PULL/TOCNs/Ag composite films with various Ag contents (0-5 wt.%). (TOCNs concentration=5 wt.%, PULL concentration=10 wt.%). (For interpretation of the references to colour in this figure legend, the reader is referred to the web version of this article.)

50 % R.H.) for up to 96 h. The weight variation from the dry condition throughout the thermal and normal exposure is shown in Figure 11. As usual, a clear continuous weight loss trend with the thermal exposure time and temperature is observed. In addition, a considerable difference in weight loss is observed owing to an increase in the temperature from 40 °C to 100 °C; however, no significant difference is observed with the addition of TOCNs and AgNPs into the PULL matrix (Figures 11a-f).

The color variation of the prepared neat PULL and PULL/

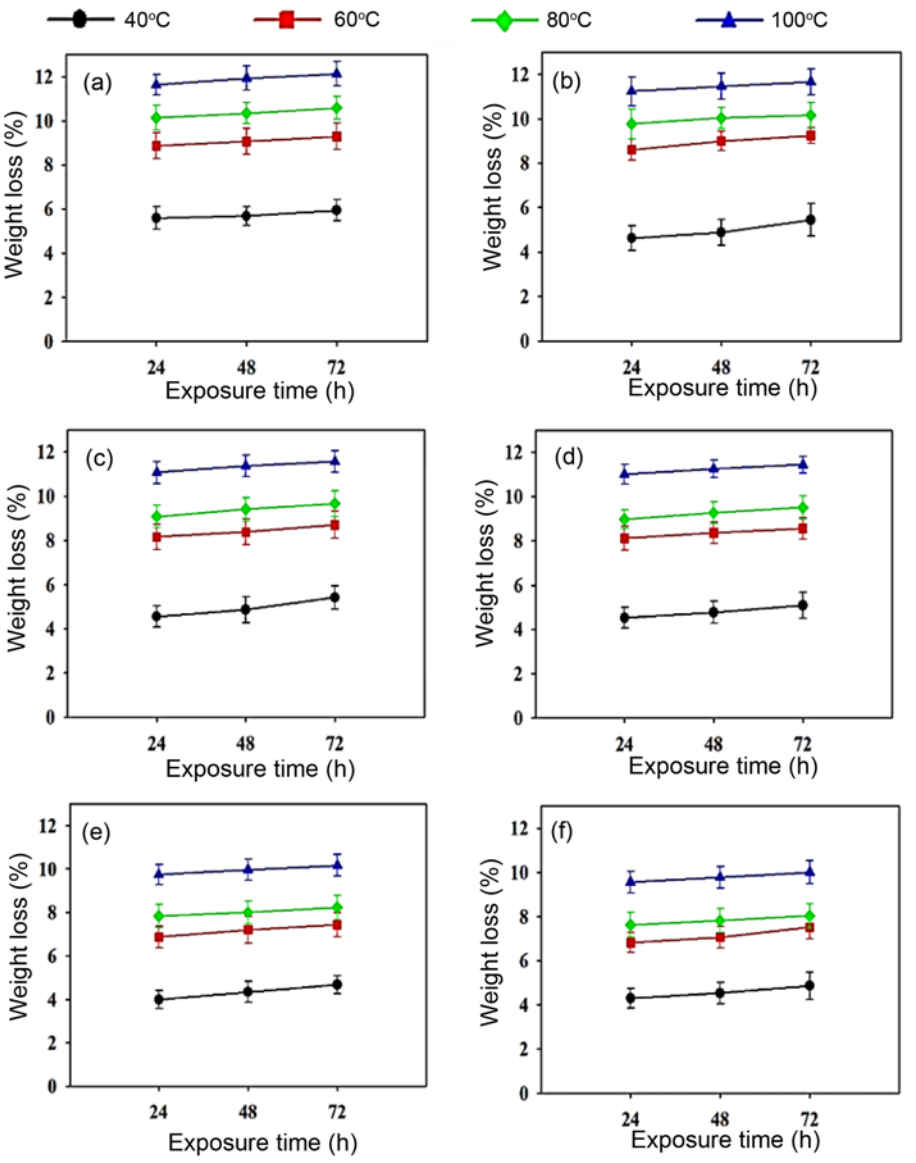

Figure 11. Weight loss results of film samples after thermal exposure; (a) PULL, (b) PULL/TOCNs, (c) PULL/TOCNs/Ag 0.5 wt.%, (d) PULL/TOCNs/Ag 1 wt.%, (e) PULL/TOCNs/Ag 3 wt.%, and (f) PULL/TOCNs/Ag 5 wt.%. (PULL concentration=10 wt.%, TOCNs concentration=5 wt.%, exposure temperature=40-100 °C).

TOCNs/Ag (0-5 %) film after 72 h thermal exposure is shown in Figure 12. A slight change in color is observed from 40 °C to 100 °C.

Tensile Strength

Figure 13 shows the tensile strength of the PULL/TOCNs/Ag film with various Ag content (0, 0.5, 1, 3, and 5 wt.%). It is determined that the tensile strength of PULL/TOCNs is improved with the addition of AgNPs. The maximum tensile strength (46.09 MPa) is determined for 5 wt.% AgNPs. Furthermore, TOCN addition also shows an improvement in tensile strength [67]. The increased mechanical improvement can be explained that the interaction between AgNPs and PULL/TOCNs has occurred; it is observed from the OM image that the film structure with AgNPs is more compact. In addition, AgNPs possessed favorable intrinsic mechanical properties. Therefore, the addition of AgNPs contributed to the increase of mechanical properties of the PULL/TOCNs film. The significant effect of Ag content on the strength of composite materials has been confirmed previously [63,68,69].

Optical Properties

Pullulan is a well-known neutral polysaccharide containing a repeating unit of D glucose, which is linked by α-1, 6 and

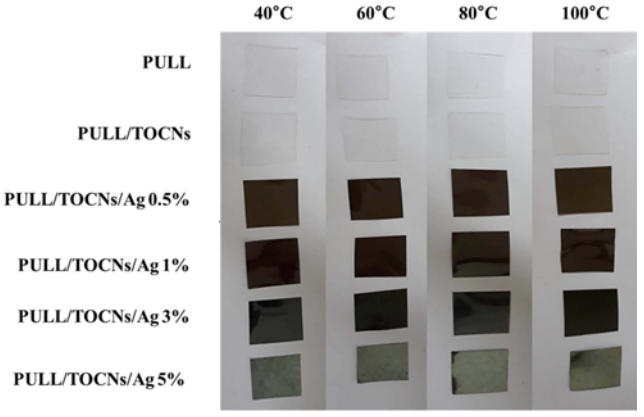

Figure 12. Color variation of neat PULL and PULL/TOCNs/Ag (0-5 %) film samples after thermal exposure at different temperatures (40-100 °C) (Exposure time=72 h).

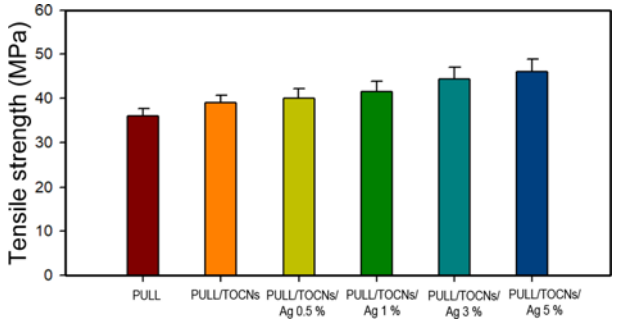

Figure 13. Tensile strength of PULL/TOCN-based nanocomposite films as a function of Ag content (TOCNs concentration=5 wt.%, PULL concentration=10 wt.%). A minimum of three specimens were tested for each sample.

Table 2. Visible light transmittance of PULL/TOCNs/Ag nanocomposite films as a function of Ag content

Sample	Visible (600 nm) T(%)
PULL	91.76±0.62
PULL/TOCNs	91.52±0.12
PULL/TOCNs/Ag 0.5 %	0.59±0.28
PULL/TOCNs/Ag 1 %	0.57±0.45
PULL/TOCNs/Ag 3 %	0.53±0.42
PULL/TOCNs/Ag 5 %	0.48±0.311

α-1, 4-glycosidic bonds [70,71]. This unique mechanical structure allows pullulan to dissolve in water without gelation at relatively high concentrations, whereas most natural polysaccharides exhibit gelation at high concentration and low temperature. Thus, hard transparent films of pullulan can be prepared by removing water [72]. Currently, pullulan is a promising material for optical applications [73,74]. Pullulan is a bio and environmentally friendly material compared to other amorphous polymers used as

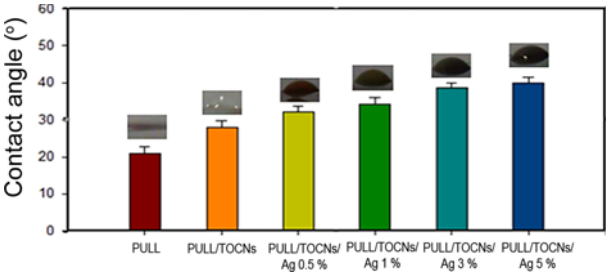

Figure 14. Water contact angle of PULL and PULL/TOCN-based nanocomposite films as a function of Ag content.

optical materials [70]. The transparency value (T%) is shown in Table 2 for the visible light wavelength (600 nm), which provides information about the filler's distribution within the matrix. The transparency rate of PULL is 91.76 % at 600 nm. The composite film with 5 wt.% TOCNs exhibited an almost the same light transmittance (91.52 %) as that of a pure PULL. However, with the addition of AgNPs (0.5-5 wt.%), the light transmittance rate decreased to 0.59, 0.57, 0.53, and 0.48 %. Thus, transparency decreases with an increase in Ag. In addition, Ag is well-dispersed within the matrix.

Water Contact Angle Measurement

To examine the surface properties of PULL/TOCNs/Ag (0-5 wt.%), contact angle measurements were conducted and are shown in Figure 14. The obtained results show that the contact angle of PULL/TOCNs/Ag (0-5 wt.%) composite films were higher than those of the neat PULL film. These results demonstrate that the neat PULL film surface polarity decreases after the addition of TOCNs and AgNPs. Yet, all elements (PULL, TOCNs, and AgNPs) in this composites film have hydrophilic ionic groups, and there are no hydrophobic surfaces. Therefore, the contact angle increase can be explained in terms of surface roughness and/or some other causes other than the chemical structure of the film [75]. A similar tendency was observed for composite film faces opposite to the petri dish; however, the contact angle values fluctuated more, most likely owing to an increase in the film surface roughness.

Moisture Uptake

One of the major drawbacks of biopolymers is water sensitivity, and the incorporation of fillers allows to overcome this problem [76]. In the present PULL/TOCNs/Ag system, the effect of TOCNs and AgNPs with various contents on water barrier properties was evaluated, and Mu values at equilibrium are shown in Figure 15. It is observed that both TOCN and AgNPs incorporation into nanocomposite exhibited a lower value of equilibrium Mu, which represents a positive effect of the fillers on the development of moisture susceptibility for PULL-based materials. Furthermore, after

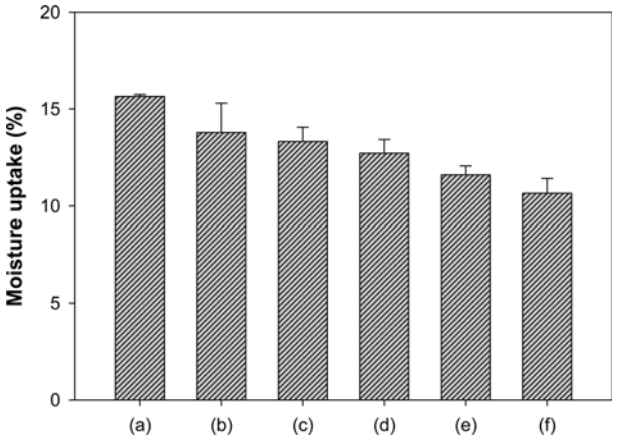

Figure 15. Moisture uptake results of (a) neat PULL, and PULL/TOCNs based nanocomposite films as a function of Ag content: (b) 0 wt.%, (c) 1 wt.%, (d) 3 wt.%, and (e) 5 wt.%.

the addition of Ag, ternary films had a more significant decline in Mu than PULL/TOCNs binary films, which showed that the incorporation of Ag and TOCNs resulted in the development of moisture resistance of PULL-based films. This occurs owing to the strong filler matrix bond stop diffusion of water molecules at the side of interfaces, which enhances water resistance. A prior study has also shown that the incorporation of AgNPs can reduce the moisture absorption of PULL [77].

Antibacterial Effectiveness

Ag nanoparticles are known to have strong inhibitory and antibacterial effects as well as a broad spectrum of antimicrobial behavior [78]. In this study, the antibacterial performance of PULL/TOCNs/Ag hybrid nanoparticles was assessed in viscous aqueous test samples, and the results are shown in Figure 16. The antibacterial efficiency of PULL/TOCNs/Ag films was evaluated by counting the total number of bacteria present in the sample as a function of storage time at 32 °C. The PULL and PULL/TOCNs films did not exhibit antibacterial performance and remained constant for a long time (Figures 16a-b). However, with the addition of PULL/TOCNs/Ag films into the test sample, a significant decrease in the bacteria number is observed. Moreover, the bacteria inhibiting rate increases with an increase in the AgNPs content (Figures 16c-f). Most of the initially inoculated bacteria could be sterilized within 7 d. This result shows that PULL/TOCNs/Ag films have an antibacterial action.

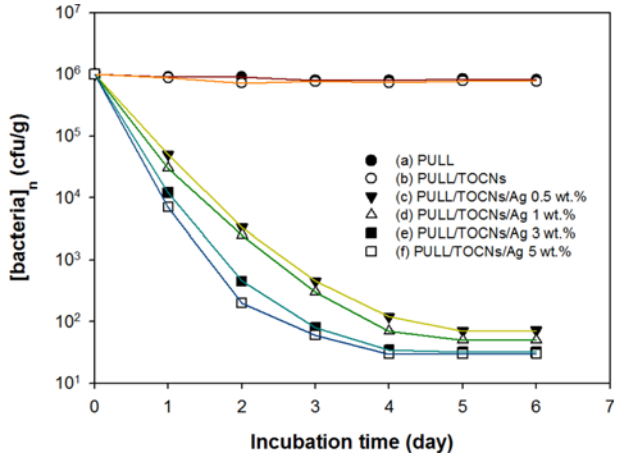

Figure 16. Preservation performance of the film samples; (a) PULL, (b) PULL/TOCNs, (c) PULL/TOCNs/Ag 0.5 wt.%, (d) PULL/TOCNs/Ag 1 wt.%, (e) PULL/TOCNs/Ag 3 wt.%, and (f) PULL/TOCNs/Ag 5 wt.% (PULL concentration=10 wt.%, TOCNs concentration=5 wt.%).

Biodegradability

PULL/TOCNs/Ag composite films were exposed to microbial attack by soil burial. Figure 17 shows that sample morphology considerably changed after 2, 4, and 16 d of soil burial. After 2 d of soil burial, the composite films were easily moistened by the soil and became pasty owing to the hydrophilic nature of the PULL matrix. Owing to the pasty and swollen surface of the film, clay can be easily adsorbed to the surface, which allows microorganisms to easily stick to the film surface. The degradation of the composite film progressed with an increase in the soil burying time. After 8 d of degradation, no continuous fragments were visible in the case of PULL and PULL/TOCNs, and Ag-containing films showed a slightly slower degradation. This result is obtained owing to the strong interaction between the PULL matrix and Ag particles [66], which enhance the cohesiveness of the pull matrix and result in reduced water sensitivity. The

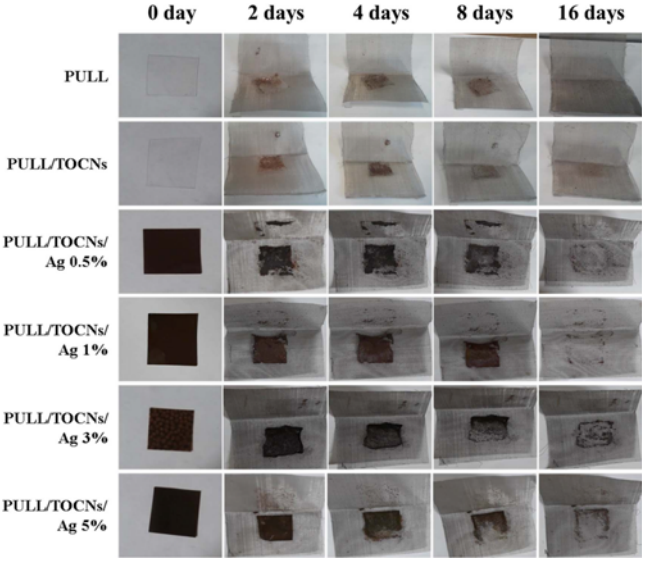

Figure 17. Macroscopic images of the biodegradation of different film samples in soil.

negative effect of Ag on the biodegradation process is also supported by other studies [79]. After 16 d, almost all films, including Ag-containing films, completely degraded. Likewise, the incorporation of TOCNs slows down the biodegradation rate of the PULL matrix up to 4 d. This result is obtained owing to the strong interaction that exists between the matrix and the filler as well as the uniform dispersion of TOCN particles in the PULL matrix. Similar findings are also observed by the other researchers [80].

Conclusion

PULL/TOCNs/Ag composite films can be prepared with different AgNPs contents (0, 0.5, 1, 3, and 5 wt.%), 10 wt.% pullulan, and 5 wt.% TOCNs by the solution casting method. Ag considerably affects the surface morphology and roughness of the PULL/TOCNs/Ag composite film. This study reveals that the incorporation of TOCNs and Ag results in a considerable improvement in the tensile strength of the PULL matrix due to the interaction among PULL, TOCNs and AgNPs. XRD patterns and OM images indicate the coexistence of PULL, TOCNs, and Ag in the studied Ag content range. A DSC thermogram showed that the PULL polymer containing Ag considerably affected the melting behavior. TGA analysis confirmed the thermal property enhancement of the composite film. The possible interactions between Ag and PULL, as well as TOCNs and the PULL matrix, are indicated by FT-IR results. In addition, it is determined that the tested PULL/TOCNs/Ag composite film is highly biodegradable; after 16 d of soil burial, almost all types of films, including those containing Ag, completely degraded. Furthermore, the prepared composite film exhibits a moisture resistance property. Moreover, the PULL films become more nonpolar after the addition of TOCNs and Ag. In addition, a continuous weight loss with an increase in exposure time and temperature was observed. During the preservation test, the prepared composite films were confirmed to be excellent antibacterial materials. These results provide a new perspective for the use of these films in real life.

Acknowledgments

This study was supported by Basic Science Research Program through the National Research Foundation of Korea (NRF) funded by Ministry of Education (NRF-2016R1A2B4010329), Korea.

References

1. R. S. Singh, N. Kaur, V. Rana, and J. F. Kennedy, *Carbohydr. Polym.*, **171**, 102 (2017).
2. S. Farris, I. U. Unalan, L. Introzzi, J. M. Fuentes-Alventosa, and C. A. Cozzolino, *J. Appl. Polym. Sci.*, **131**, 40539 (2014).
3. R. S. Singh, N. Kaur, V. Rana, and J. F. Kennedy, *Carbohydr. Polym.*, **153**, 455 (2016).
4. R. S. Singh, N. Kaur, and J. F. Kennedy, *Carbohydr. Polym.*, **123**, 190 (2015).
5. M. Gniewosz and A. Synowiec, *Flavour Frag. J.*, **26**, 389 (2011).
6. H.-K. Mahbobeh, K. Faramarz, and S.-G. Iman, *J. Food Sci. Technol.*, **53**, 1294 (2016).
7. N. Kandemir, A. Yemeniciogwlu, Ç. Mecitogwlu, Z. S. Elmaci, A. Arslanogwlu, Y. Göksungur, and T. Baysal, *Food Technol. Biotechnol.*, **43**, 343 (2005).
8. M. K. Morsy, H. H. Khalaf, A. M. Sharoba, H. H. El-Tanahi, and C. N. Cutter, *J. Food Sci.*, **79**, M675 (2014).
9. R. J. Pinto, A. Almeida, S. C. Fernandes, C. S. Freire, A. J. Silvestre, C. P. Neto, and T. Trindade, *Colloid Surf. B-Biointerfaces*, **103**, 143 (2013).
10. L. C. Tomé, N. H. Silva, H. R. Soares, A. S. Coroadinha, P. Sadocco, I. M. Marrucho, and C. S. Freire, *Green Chem.*, **17**, 4291 (2015).
11. V. Trinetta, J. D. Floros, and C. N. Cutter, *J. Food Saf.*, **30**, 366 (2010).
12. E. Trovatti, S. C. Fernandes, L. Rubatat, D. da Silva Perez, C. S. Freire, A. J. Silvestre, and C. P. Neto, *Compos. Sci. Technol.*, **72**, 1556 (2012).
13. E. Trovatti, S. C. Fernandes, L. Rubatat, C. S. Freire, A. J. Silvestre, and C. P. Neto, *Cellulose*, **19**, 729 (2012).
14. I. U. Unalan, C. Wan, Ł. Figiel, R. T. Olsson, S. Trabattoni, and S. Farris, *Nanotechnology*, **26**, 275703 (2015).
15. C. Zhang, D. Gao, Y. Ma, and X. Zhao, *J. Food Sci.*, **78**, C805 (2013).
16. Y. Nishiyama, *J. Wood Sci.*, **55**, 241 (2009).
17. I. M. Saxena and R. M. Brown Jr, *Ann. Bot.*, **96**, 9 (2005).
18. I. Sakurada, Y. Nukushina, and T. Ito, *J. Polym. Sci.*, **57**, 651 (1962).
19. S. Iwamoto, A. N. Nakagaito, H. Yano, and M. Nogi, *Appl. Phys. A-Mater. Sci. Process.*, **81**, 1109 (2005).
20. A. N. Nakagaito and H. Yano, *Appl. Phys. A-Mater. Sci. Process.*, **80**, 155 (2005).
21. A. J. Svagan, M. A. S. Azizi Samir, and L. A. Berglund, *Biomacromolecules*, **8**, 2556 (2007).
22. M. A. S. Azizi Samir, F. Alloin, and A. Dufresne, *Biomacromolecules,* **6**, 612 (2005).
23. X. M. Dong, J.-F. Revol, and D. G. Gray, *Cellulose,* **5**, 19 (1998).
24. A. Dufresne, J. Y. Cavaillé, and W. Helbert, *Polym. Compos.*, **18**, 198 (1997).
25. S. J. Eichhorn, *Soft Matter.*, **7**, 303 (2011).
26. W. Helbert, J. Cavaille, and A. Dufresne, *Polym. Compos.*, **17**, 604 (1996).
27. H. Liu, D. Liu, F. Yao, and Q. Wu, *Bioresour. Technol.*, **101**, 5685 (2011).
28. R. H. Marchessault, F. F. Morehead, and N. M. Walter, *Nature*, **184**, 632 (1959).
29. A. Llorens, E. Lloret, P. A. Picouet, R. Trbojevich, and A. Fernandez, *Trends Food Sci. Technol.*, **24**, 19 (2012).

30. D. S. Cha and M. S. Chinnan, *Crit. Rev. Food Sci. Nutr.*, **44**, 223 (2004).
31. V. Falguera, J. P. Quintero, A. Jiménez, J. A. Muñoz, and A. Ibarz, *Trends Food Sci. Tech.*, **22**, 292 (2011).
32. L. Bi, L. Yang, G. Narsimhan, A. K. Bhunia, and Y. Yao, *J. Control. Release*, **150**, 150 (2011).
33. N. Cioffi, L. Torsi, N. Ditaranto, G. Tantillo, L. Ghibelli, L. Sabbatini, T. Bleve-Zacheo, M. D'Alessio, P. G. Zambonin, and E. Traversa, *Chem. Mat.,* **17**, 5255 (2005).
34. S.-I. Hong and J.-W. Rhim, *J. Nanosci. Nanotechnol.*, **8**, 5818 (2008).
35. J.-W. Rhim, S.-I. Hong, H.-M. Park, and P. K. Ng, *J. Agric. Food Chem.*, **54**, 5814 (2006).
36. X. Wang, Y. Du, J. Yang, X. Wang, X. Shi, and Y. Hu, *Polymer*, **47**, 6738 (2006).
37. P. Sanpui, A. Murugadoss, P. D. Prasad, S. S. Ghosh, and A. Chattopadhyay, *Int. J. Food Microbiol.*, **124**, 142 (2008).
38. R. Yoksan and S. Hirachanchai, *Mater. Sci. Eng. C*, **30**, 891 (2010).
39. S. Liau, D. Read, W. Pugh, J. Furr, and A. Russell, *Lett. Appl. Microbiol.*, **25**, 279 (1997).
40. A. Russell and W. Hugo, "7 Antimicrobial Activity and Action of Silver. In Progress in Medicinal Chemistry", pp.351-370, Elsevier, 1994.
41. A. Emamifar, M. Kadivar, M. Shahedi, and S. Soleimanian-Zad, *Food Control*, **22**, 408 (2011).
42. N. H. Silva, C. Vilela, A. Almeida, I. M. Marrucho, and C. S. Freire, *Food Hydrocolloids*, **77**, 921 (2018).
43. Q. Xiao, K. Lu, Q. Tong, and C. Liu, *J. Food Process Eng.*, **38**, 155 (2015).
44. M. Kaur, M. Arshad, and A. Ullah, *ACS Sustainable Chem. Eng*., **6**, 1977 (2018).
45. E. Barnes, J. A. Jefcoat, E. M. Alberts, M. A. McKechnie, H. R. Peel, J. P. Buchanan, C. A. Weiss Jr., K. L. Klaus, L. C. Mimun, and C. M. Warner, *Polymers*, **11**, 1091 (2019).
46. T. Kurihara and A. Isogai, *Cellulose*, **21**, 291 (2014).
47. S. Yeasmin, J. H. Yeam, and S. B. Yang, *Carbohydr. Polym.*, **240**, 116307 (2020).
48. S. Yeasmin, J. H. Yeum, B. C. Ji, J. H. Choi, and S. B. Yang, *Nanomaterials*, **11**, 602 (2021).
49. A. Doblies, B. Boll, and B. Fiedler, *Polymers,* **11**, 363 (2019).
50. J. K. Farrington, E. L. Martz, S. J. Wells, C. C. Ennis, J. Holder, J. W. Levchuk, K. E. Avis, P. S. Hoffman, A. D. Hitchins, and J. M. Madden, *Appl. Environ. Microb.*, **60**, 4553 (1994).
51. S. Chuayjuljit, S. Hosililak, and A. Athisart, *J. Met. Mater. Miner.*, **19**, 59 (2009).
52. E. Chong, S. Jafarzadeh, M. Paridah, D. A. Gopakumar, H. Tajarudin, S. Thomas, and H. Abdul Khalil, *Polymers*, **11**, 210 (2019).
53. O. Ochoa-Yepes, L. Di Giogio, S. Goyanes, A. Mauri, and L. Famá, *Carbohydr. Polym.*, **208**, 221 (2019).
54. K. Katerinopoulou, A. Giannakas, N. M. Barkoula, and A. Ladavos, *Starch-Stärke,* **71**, 1800076 (2019).
55. H. Lu, S. A. Madbouly, J. A. Schrader, G. Srinivasan, K. G. McCabe, D. Grewell, R. K. Michael, and W. R. Graves, *ACS Sustain. Chem. Eng.*, **2**, 2699 (2019).
56. Z. Wu, W. Deng, J. Luo, and D. Deng, *Carbohydr. Polym.*, **205**, 447 (2019).
57. H.-P. Seo, C.-W. Son, C.-H. Chung, D.-I. Jung, S.-K. Kim, R. A. Gross, D. L. Kaplan, and J.-W. Lee, *Bioresour. Technol.*, **95**, 293 (2004).
58. P. Eronen, K. Junka, J. Laine, and M. Österberg, *BioResources*, **6**, 4200 (2011).
59. Y. Ishimaru and T. Lindström, *J. Appl. Polym. Sci.*, **29**, 1675 (1984).
60. E. Sjostrom, "Wood Chemistry: Fundamentals and Applications", Gulf Professional Publishing, 1993.
61. C. G. Biliaderis, A. Lazaridou, and I. Arvanitoyannis, *Carbohydr. Polym*., **40**, 29 (1999).
62. M. R. Karim, H. W. Lee, R. Kim, B. C. Ji, J. W. Cho, T. W. Son, W. Oh, and J. H. Yeum, *Carbohydr. Polym.*, **78**, 336 (2009).
63. M. M. Abutalib and A. Rajeh, *Polym.Test.*, **93**, 107013 (2021).
64. E. Alsharaeh, *Materials,* **9**, 458 (2016).
65. D. Poudel, S. Swilley-Sanchez, S. O'keefe, J. Matson, T. Long, and C. Fernández Fraguas, *Polymers*, **12**, 2558 (2020).
66. M. S. Islam and J. H. Yeum, *Colloid Surf. A-Physicochem. Eng. Asp.*, **436**, 279 (2013).
67. S. Fujisawa, T. Ikeuchi, M. Takeuchi, T. Saito, and A. Isogai, *Biomacromolecules,* **13**, 2188 (2012).
68. X. Pan, H. Gao, Y. Su, Y. Wu, X. Wang, J. Xue, T. He, Y. Lu, J. Liu, and S. Yu, *Nano Res.*, **11**, 410 (2018).
69. C.-H. Su, H.-L. Chen, S.-P. Ju, H.-Y. Chen, C.-W. Shih, C.-T. Pan, and T.-D. You, *Sci. Rep*., **10**, 7600 (2020).
70. J.-I. Horinaka, Y. Hashimoto, and T. Takigawa, *Int. J. Biol. Macromol.*, **118**, 584 (2018).
71. S. Ueda and H. Kono, *Appl. Environ. Microbiol.*, **13**, 882 (1965).
72. T. D. Leathers, *Appl. Microbiol. Biotechnol.*, **62**, 468 (2003).
73. T. Danjo, Y. Enomoto, H. Shimada, S. Nobukawa, M. Yamaguchi, and T. Iwata, *Sci. Rep.*, **7**, 46342 (2017).
74. V. Trinetta, C. N. Cutter, and J. Floros, *LWT-Food Sci. Technol.*, **44**, 2296 (2011).
75. M. Zolfi, F. Khodaiyan, M. Mousavi, and M. Hashemi, *Carbohydr. Polym.*, **109**, 118 (2014).
76. J. Duanmu, E. K. Gamstedt, and A. Rosling, *Compos. Sci. Technol.*, **67**, 3090 (2007).
77. V. Chaurasia and S. Bajpai, *Int. J. Polym. Mater.*, **62**, 119 (2013).
78. D. P. Dowling, K. Donnelly, M. L. McConnell, R. Eloy, and M. N. Arnaud, *Thin Solid Films,* **398**, 602 (2001).
79. V. Lazić, M. Radoičić, Z. Šaponjić, T. Radetić, V. Vodnik, S. Nikolić, S. Dimitrijević, and M. Radetić, *Cellulose,* **22**, 1365 (2015).
80. B. Deepa, E. Abraham, L. Pothan, N. Cordeiro, M. Faria, and S. Thomas, *Materials,* **9**, 50 (2016).